Retrospective voxel-based dosimetry for assessing the body surface area model ability to predict delivered dose and radioembolization outcome

Marilyne Kafrouni[1,2,6]**, Carole Allimant**[3]**, Marjolaine Fourcade**[1]**, Sébastien Vauclin**[2]**, Julien Delicque**[3]**, Alina-Diana Ilonca**[1]**, Boris Guiu**[3,6]**, Federico Manna**[4]**, Nicolas Molinari**[4,6]**, Denis Mariano-Goulart**[1,5,6]**, Fayçal Ben Bouallègue**[1,5,6]

[1] Department of Nuclear Medicine, Montpellier University Hospital, Montpellier, France

[2] DOSIsoft SA, Cachan, France

[3] Department of Radiology, Montpellier University Hospital, Montpellier, France

[4] Department of Medical Information, Montpellier University Hospital, Montpellier, France

[5] PhyMedExp, INSERM, CNRS, Montpellier, France

[6] University of Montpellier, Montpellier, France.

Corresponding author:

Marilyne Kafrouni, PhD candidate

Nuclear Medicine Department, Gui de Chauliac University Hospital,
80 avenue Augustin Fliche, 34295 Montpellier Cedex 5, France

Email address: marilyne.kafrouni@gmail.com

Tel: +33467330206

Fax: +33467336922

Word count: 5049

Running title: The BSA model limitations

1

ABSTRACT

The aim of this study was to quantitatively evaluate the body surface area (BSA) model ability to predict tumor absorbed dose and treatment outcome through retrospective voxel-based dosimetry. **Methods:** Data from thirty-five hepatocellular carcinoma patients with a total of forty-two resin microsphere radioembolization treatments were included. Injected activity was planned with the BSA model. Voxel dosimetry based on ^{99m}Tc-labeled macroaggregated albumin SPECT and ^{90}Y-microsphere PET was retrospectively performed using a dedicated treatment planning system (PLANET® Dose, DOSIsoft SA, Cachan, France). Average dose and dose-volume histograms (DVHs) of the anatomically-defined tumors were analyzed. The selected dose metrics extracted from DVHs were: minimum dose to 50% and 70% of the tumor volume (D_{50} and D_{70} respectively) and percentage of the volume receiving at least 120 Gy (V_{120}). Treatment response was evaluated six months after therapy according to the European Association for the Study of the Liver (EASL) criteria. **Results:** Six month response was evaluated in 26 treatments: 14 were considered as objective response (OR) and 12 as non-responding (NR). ^{90}Y-microsphere PET based retrospective dosimetry evaluation showed a large inter-patient variability with a median average absorbed dose to the tumor of 60 Gy. In 62% (26/42) of the cases, tumor, non-tumoral liver, and lung doses could have complied with the recommended thresholds by increasing the injected activity calculated by the BSA method. Average doses, D_{50}, D_{70}, and V_{120} were significantly higher in OR than in NR. **Conclusion:** In our population, tumor average dose and DVH metrics were associated with tumor response. However the activity calculated by the BSA could have been increased to reach the recommended tumor dose threshold. Tumor uptake, target and non-target volumes, and dose distribution heterogeneity should be taken into account for activity planning.

INTRODUCTION

Today, for ^{90}Y resin microspheres (SIR-Spheres®, SIRTeX Medical, Sydney, Australia), three activity planning methods are recommended by the manufacturer: empirical model, body surface area (BSA) and partition model (*1,2*). The empirical model recommends exclusively three values of activity based on tumor involvement. The BSA method which has been historically used for chemotherapy is based on patient surface area and tumor involvement but neglects the tumor-to-normal liver (T/N) uptake ratio. The partition model is based on the Medical Internal Radiation Dose principles and is considered as more accurate and personalized. The partition model accounts for tumor avidity but assumes uniform dose distribution in the tumor. Despite its semi-empirical nature, the BSA method is the most widely used so far for its simplicity.

Many authors have discussed BSA limitations emphasizing the lack of correlation with liver volume, tumor avidity and absorbed dose and recommending more accurate and personalized methods (*3-6*). However, this was not quantitatively addressed with a voxel-based dosimetry. This study is a retrospective 3D voxel-based dosimetry analysis in a hepatocellular carcinoma (HCC) population treated by ^{90}Y-microsphere radioembolization with injected activity planned using the BSA calculation. The aim is to quantitatively evaluate BSA ability to predict tumor absorbed dose and treatment outcome.

MATERIALS AND METHODS

Patient Characteristics

A total of 42 treatments in 35 HCC patients performed at our institution by radioembolization with ^{90}Y resin microspheres from February 2012 to December 2015 were included in this study. Among the 35 patients, 23 were included in the SorAfenib versus Radioembolization in Advanced Hepatocellular carcinoma protocol. Authorization for ancillary study was duly obtained from the protocol principal investigator. All patients gave written informed consent to treatment and retrospective analysis of their clinical and imaging data for research purpose.

All patients included in this study had unresectable HCC. Baseline characteristics of the treatments are reported in Table 1. For a same patient, treatments targeting separately the right and left lobes or sequential treatments at more than a six-month interval were considered as distinct procedures. There were 1 whole-liver, 35 lobar and 6 segmental treatments. A retrospective dosimetric study was conducted on the forty-two radioembolization sessions.

3

^{99m}Tc-MAA Imaging and Activity Planning

^{99m}Tc-labeled macroaggregated albumin (^{99m}Tc-MAA) were injected into the hepatic artery as microsphere surrogate. Planar and SPECT/CT images were acquired within an hour. This simulation step was used for lung shunt fraction estimation and verification of right targeting/absence of extrahepatic deposition.

SPECT/CT data were acquired using an Infinia Hawkeye IV (GE Healthcare, Waukesha, WI, USA) with the following parameters: spectroscopic window at 140 keV ± 10%, 32 projections, 25s/projection, matrix 128 x 128, voxel size 4.4 x 4.42 x 4.42 mm^3, low energy high resolution collimator. SPECT data were reconstructed on a Xeleris 3.0562 workstation (GE Healthcare, Waukesha, WI, USA) using Ordered-Subset Expectation-Maximization with 5 iterations and 8 subsets, attenuation and scatter corrections using GE standard commercial solutions.

Activity was planned following the microsphere manufacturer recommendations at that time. Following the most recent method proposed by Kennedy *et al.* (*7*), the BSA model was applied according to the type of treatment.

For total liver treatment:

$$A\ (GBq) = BSA - 0.2 + \frac{V_{Tumour}}{V_{Total\ liver}}$$

For lobar treatment:

$$A\ (GBq) = \left(BSA - 0.2 + \left(\frac{V_{Tumour\ lobe}}{V_{Total\ lobe}}\right)\right) \times \left(\frac{V_{Total\ lobe}}{V_{Total\ liver}}\right)$$

For segment treatment:

$$A\ (GBq) = \left(BSA - 0.2 + \left(\frac{V_{Tumour\ segment}}{V_{Total\ segment}}\right)\right) \times \left(\frac{V_{Total\ segment}}{V_{Total\ liver}}\right)$$

With

$$BSA\ (m^2) = 0.20247 \times height^{0.725}(m) \times weight^{0.425}(kg)$$

With V_{Tumor} as the tumor volume, $V_{Tumor\ lobe}$ as the tumor volume in the treated lobe, $V_{Total\ lobe}$ as the lobe volume including the tumor, $V_{Tumor\ segment}$ as the tumor volume in the treated segment, $V_{Total\ segment}$ as the segment volume including the tumor, $V_{Total\ liver}$ as the total liver volume including the tumor. These volumes were previously defined by radiologists on contrast-enhanced computed tomography (CT) or magnetic resonance imaging (MRI).

Lung shunt fraction was evaluated using anterior and posterior planar scans. A dose to the lungs >25 Gy or presence of significant focal extra-hepatic uptake were considered as contraindications for treatment.

^{90}Y-microsphere Imaging

Microsphere distribution was controlled for each treatment session by a PET/CT exam on the next day. Liver-centered PET/CT acquisitions were performed on a Biograph non-TOF PET/CT (Siemens Healthcare, Erlangen, Germany) for a total scan duration of 40 min. PET reconstruction parameters used at this time for SIRT dosimetry were: 3D Ordered-Subset Expectation-Maximization (1 iteration/8 subsets) with point spread function compensation, attenuation correction, Gaussian post-filtering with full width at half maximum of 4 mm, 128×128 matrix with a voxel size of 5.3×5.3×3.4 mm^3.

Retrospective Dosimetry

Retrospective ^{99m}Tc-MAA SPECT and ^{90}Y-microsphere PET based voxel dosimetry were performed using a treatment planning system (PLANET® Dose, DOSIsoft SA, Cachan, France) following a process similar to the one used in external beam radiation therapy (Figure 1).

The first step was the anatomical segmentation of target volumes (considered as one global unique volume) and whole liver volume on contrast-enhanced CT or MRI images. This was done by a single radiologist using the diagnostic workstation available in the radiology department (AW Workstation, GE Healthcare, Waukesha, WI, USA). When relevant (n=2), necrotic (i.e., non-enhancing) area was subtracted from the tumor volume to assess dose in the viable tumor only. Contours were then imported as RT-Struct sets in the treatment planning system. Lesions <2 cm were not considered for dose assessment in order to limit partial volume effect induced bias. The non-tumoral liver (NTL) volume was defined in the treatment planning system by subtracting the tumor volume from the total liver volume.

^{99m}Tc-MAA SPECT/CT and ^{90}Y-microsphere PET/CT images were co-registered with the reference exam (contrast-enhanced CT or MRI). ^{99m}Tc-MAA SPECT images were normalized so that total hepatic uptake matches the actual therapeutic activity corrected for lung shunt fraction and residual activity.

3D dose map was calculated for pre- and post-treatment dosimetry using a kernel convolution algorithm at voxel level based on the Medical Internal Radiation Dose formalism detailed in Pamphlet No. 17 (*8*). Dose to a given target voxel k from N surrounding source voxels h (including the target voxel itself, h=0) is given by the equation:

5

$$D(voxel_k) = \sum_{h=0}^{N} \tilde{A}_{(voxel_h)} \times S(voxel_k \leftarrow voxel_h)$$

where $\tilde{A}_{(voxel)h}$ is the time-integrated activity within voxel h and $S(voxel_k \leftarrow voxel_h)$ is the absorbed dose per unit cumulated activity between each voxel pair (S-value). This was implemented in the dose calculation algorithm as a discrete convolution between the time-integrated activity map containing each individual $\tilde{A}_{(voxel_h)}$ and the voxel S-value kernel.

Average dose to the tumor (D_{avg}) and metrics extracted from dose-volume histograms (DVH): the minimum dose to 50% and 70% of the tumor volume (D_{50} and D_{70} respectively) and the percentage of the volume receiving at least 120 Gy (V_{120}) were studied.

Therapy response

Treatment response was evaluated on follow-up contrast-enhanced CT or MRI obtained six months after radioembolization in blind analysis by two radiologists. Response was defined according to the recommendations of the European Association for the Study of the Liver (EASL) (*9*). Tumor response was conventionally classified as: complete response (CR) for absence of any enhancing tissue, partial response for a ≥50% decrease in enhancing tissue, progressive disease (PD) for a ≥25% increase in the size of one or more measurable lesions or appearance of new lesions, and stable disease (SD) otherwise. Objective response (OR) was defined as either CR or partial response. SD or PD were considered as non-responding (NR).

Statistical analysis

The optimal to actual (BSA-planned) activity ratio was calculated for each evaluation based on ^{90}Y-microsphere PET dosimetry. Optimal activity was defined as the injected activity that would enable to meet the tumor, NTL, and lung dose criteria of ≥120 Gy, <50 Gy and <30 Gy respectively as reported in the literature (*7,10*). For each case, the ratio lower bound corresponds to an optimal injected activity that would enable to deliver 120 Gy to the tumor. The ratio upper bound represents the maximal activity complying with the 50 Gy limit to the NTL and the 30 Gy limit to the lungs. When the activity ratio based on the NTL or lung threshold was lower than the ratio based on the tumor threshold, only the NTL or lung tolerance criteria was taken into account.

Dose metrics based on ^{99m}Tc-MAA SPECT and ^{90}Y-microsphere PET were compared using paired Student's *t* test. ^{90}Y-microsphere based dose metrics in OR and NR were compared using Student's *t* test. Pearson's

6

correlation and Bland-Altman analysis were used to evaluate the agreement between optimal activities based on ^{99m}Tc-MAA and ^{90}Y-microsphere dosimetry. A P-value ≤0.05 was considered as significant.

RESULTS

Therapy response

Treatment response assessment was available six months after therapy in 26 treatments because of early deaths that occurred before six months (n=16). The six month response rate according to EASL criteria evaluated on these 26 treatments was 54%. There were 14 OR including 4 CR and 10 partial responses, and 12 NR including 5 SD and 7 PD. For one patient, response was considered as CR because he was down-staged and benefited from a hepatectomy four months after radioembolization.

Dosimetry

Table 2 summarizes the main dosimetric data over the analyzed treatments: injected activity (IA), lung shunt fraction, treated tumor volume (V_T), average dose to the tumor and to the NTL, D_{70}, D_{50} and V_{120}. Dose variable subscripts refer to ^{99m}Tc-MAA SPECT and ^{90}Y-microsphere PET based dosimetry. Average dose to the tumor and all DVH indices based on ^{90}Y-microsphere PET dosimetry were significantly higher in OR than in NR (97±53 Gy vs 60±24 Gy for D_{avg}, 87±49 Gy vs 50±21 Gy for D_{50}, 61±38 Gy vs 34±17 Gy for D_{70}, and 28±28 % vs 9±13 % for V_{120}). Difference between ^{99m}Tc-MAA SPECT and ^{90}Y-microsphere PET based dosimetry was not significant for all metrics except the average dose to the NTL.

Figure 2 shows the distribution of ^{90}Y-microsphere PET based tumor mean dose and DVH metrics in NR and OR treatments. Number and percentage of responding tumors are specified for stratified ranges of each dose metric, highlighting dose-effect relationship.

Looking at the average dose to the tumor, for $D_{avg-90Y}$≥120 Gy, all treatments (n=4) were evaluated as responding (OR). On the contrary, when $D_{avg-90Y}$≤40 Gy all treatments (n=3) were in a PD state. For intermediate values of $D_{avg-90Y}$ ranging from 44 Gy to 105 Gy, treatments were in OR (n=10), SD (n=5) or PD (n=4) states.

When D_{70-90Y}≥80 Gy, all treatments (n=3) were considered as OR with a $D_{avg-90Y}$ from 93 Gy to 180 Gy. When D_{70-90Y}≤ 20 Gy, which means 30% of the volume receiving less than 20 Gy, all treatments (n=2) were in PD state with

7

$D_{avg\text{-}90Y}$ from 24 Gy to 34 Gy. For intermediate values of $D_{70\text{-}90Y}$ ranging from 23 Gy to 69 Gy, treatments were in OR (n=11), SD (n=5) or PD (n=5) states.

Optimal activity

For each of the 42 treatments, the optimal activity to reach a dose of 120 Gy to the tumor was calculated using proportionality relationship based on ^{90}Y-microsphere dosimetry and ranged from 0.43 to 7.8 GBq. Adding the 50 Gy and 30 Gy limits to the NTL and lungs respectively, the optimal activity ranged from 0.43 to 6.9 GBq.

The ratio of the optimal activity to the activity planned by the BSA model was calculated for each of the 26 treatments evaluated at 6 months. Figure 3 shows the ratio values according to tumor response. The ratio to reach an average dose of 120 Gy to the tumor while keeping the dose to the NTL and the lungs under the tolerance thresholds were significantly higher in the NR group (2.3±1.1; range 1.1–5.1) than in the OR group (1.4 ± 0.6; range 0.6–2.7; *P*=0.03). In 73% of the treatments (19/26), 120 Gy to the tumor could have been delivered while keeping the dose to the NTL and lungs less than 50 Gy and 30 Gy respectively. Considering all treatments, this proportion was 62% (26/42). In the remaining treatments, the 120 Gy objective would not have been achievable because of unfavorable tumor targeting.

Figure 4 shows the results regarding the comparison (correlation plot and Bland-Altman diagram) between ^{99m}Tc-MAA SPECT and ^{90}Y-microsphere PET based optimal activities. There was an overall good agreement between the two dosimetric approaches (Pearson's R=0.86, *P*<0.001).

DISCUSSION

Therapy response

Tumor response was assessed according to EASL criteria as recommended in the literature. Keppke *et al.* showed that using combined criteria (size and necrosis) is more accurate for response assessment after radioembolization than using criteria only based on size (*11*). Six-month evaluation was chosen since full response after radioembolization is supposed to be assessable 4-8 months after therapy (*12*).

In this study, 3D dose delivered to the tumor was retrospectively evaluated showing two main results regarding the BSA method and dose-effect relationship.

The BSA: a non-dosimetry approach

The first result is related to an overall analysis of delivered doses when activity was planned with the more recent version of the BSA method described by Kennedy *et al.* (*7*). In the literature, the recommended dose to be delivered to HCC tumors to achieve response with ^{90}Y resin microsphere radioembolization is 120 Gy (*10*). In our population, the median value of the average dose was 60 Gy which is half the recommended dose and in only six cases (14% of the treatments), the tumor average dose was higher than the 120 Gy objective. As for the doses to the NTL, they were all lower than the 50 Gy threshold. Furthermore, for 26 over 42 treatments (62% of the treatments), 120 Gy to the tumor could have been delivered while keeping the dose to the NTL and to the lungs less than 50 Gy and 30 Gy respectively. The under-dosing retrospectively observed in most of the cases could be related to the BSA calculation used which is not a "dosimetry based" method, like Kao *et al.* mentioned (*3*). This is illustrated by Figure 3 where the optimal IA would be higher than the IA planned by the BSA model for all the treatments evaluated as NR (ratio>1). In the remaining 38% of the treatments, the 120 Gy objective would not have been achievable because of unfavorable tumor targeting.

More recently, Kao *et al.* discussed the limitations of the BSA method by pointing out particularly the missing T/N ratio in the BSA formula (*13*). T/N ratio referring to the preferential microsphere implantation in the tumor is lesion-based and underlies radioembolization efficacy. Low dose values are precisely due to non-favorable T/N ratio. Neglecting T/N ratio could partly explain the high inter-patient variability in absorbed doses ($D_{avg-90Y}$ = 74±47 Gy; range 23–197 Gy) while the same planning objective was assumed when applying the BSA. Also, as noted by several authors the BSA is not correlated to the liver size. This may be suitable in a healthy population but can lead to over or under dosage for cancerous livers, especially in situations of extreme tumor burden (*5,14,15*) or atrophic liver related to chronic liver disease.

Moreover, Kao *et al.* interestingly noted that being based only on patient height, weight and tumor involvement, the range of activities calculated by the BSA method would mainly be included between 1 and 3 GBq when considering extreme cases (*3*). In our population, to reach the 120 Gy mean absorbed dose to the tumor while keeping the dose to the NTL and the lungs below the 50 Gy and 30 Gy tolerance thresholds, IA should have ranged from 0.43 to 6.5 GBq. This range of activity values exceeds the activity vials available today. These theoretical values would need to be adjusted taking into account other factors such as patient baseline condition, remaining hepatic

9

function, and tumor uptake (1), hence multiplying the activity by a simple coefficient would likely not be adequate in most of the cases. The flaw is in the BSA formula itself which is not adapted for this therapy since it disregards essential parameters such as T/N ratio, liver volume and dose distribution heterogeneity. Today, only voxel-based dosimetry integrates all these variables and its feasibility has already been proven ($16,17$).

Dose-effect relationship

The second interesting result is the relationship between dose and treatment response for HCC patients. Average dose and all dose metrics extracted from DVHs were significantly higher in the OR compared to the NR (Table 2).

Although the average value of D_{70-90Y} was 45 Gy over the treatments we analyzed, it can be noted that for D_{70-90Y} higher than 80 Gy all treatments resulted in OR (n=3). Kao $et\ al.$, who were ones of the earliest authors to analyze DVHs for ^{90}Y-microsphere radioembolization, suggested $D_{70} > 100$ Gy for CR (18). Putting aside differences in terms of methodology applied, discrepancies between the two thresholds can be explained by the fact that delivered doses were higher in their population and patients were selected as treated under highly favorable conditions. In both studies, this DVH analysis was carried out in a few number of patients. A larger study is required to define dose thresholds from DVH as additional dosimetric indicators to the average dose commonly used. In agreement with tumor dose objective given in the literature, all tumors (n=4) receiving an average dose higher than 120 Gy were evaluated as responding to treatment (10).

Therefore, combining average dose value and dose metrics extracted from DHVs could help to plan the suitable therapeutic activity and predict treatment response.

Like reported by several authors, both the BSA and the partition model are based on the assumption of homogeneous microsphere deposition ($6,19$). However, as Kao $et\ al.$ pointed out, many studies have shown microsphere deposition heterogeneity at microscopic and macroscopic levels ($3,19$-22). For this reason, interest for voxel-based dosimetry is growing for predicting tumor control as D'Arienzo $et\ al.$ concluded on their case report (23). In addition to greater accuracy, dose map calculation provides similar analysis tools as the ones used in external beam radiation therapy to help the medical team for treatment planning optimization: dose profiles, isodose displays, DVHs, etc.

Limitations and perspectives

Caution should be taken with dose values given here only on an indicative basis to highlight dose-effect relationship. They cannot be considered as dose thresholds applicable in a clinical context due to two main limitations. First, a limited number of patients was included in order to ensure the homogeneity of the cohort in terms of tumor histology, microsphere type, and planning methodology. Second, ^{90}Y-microsphere PET based dosimetry may suffer with variability due to image noise and free-breathing acquisition, as well as bias related to partial volume effect and registration inaccuracies.

In this study, tumor dosimetry based on ^{99m}Tc-MAA was not significantly different from the one based on ^{90}Y-microsphere. Although MAA is not a perfect microsphere surrogate as already discussed in the literature (*24,25*), it is today the only consensual method to assess dose before treatment and it plays a key role in planning the activity to inject. That is why the agreement between ^{99m}Tc-MAA SPECT and ^{90}Y-microsphere PET dosimetry needs to be investigated in more detail.

As it appears on Figure 3, there was in most of the cases a wide margin of decision between the two classical approaches discussed in the literature, i.e. the "minimal efficient activity" (preserving the NTL as much as possible while delivering sufficient dose to the tumor) (*10*) and the maximal tolerable activity (*26*). Individual therapeutic decision requires a patient-based approach taking into account patient clinical status, hepatic functional reserve, as well as cumulative dose issues if future therapies are considered.

CONCLUSION

This retrospective study highlighted two main results. First, the activity to administer calculated by the BSA method could have been increased in most of the cases to comply with the dose thresholds recommended in the literature. Second, in our population, tumor dosimetry (whether in terms of average dose or DVH metrics) was markedly associated with tumor response. The increasing interest for radioembolization is going to require dosimetry tools and reference levels to be able to better personalize treatments.

COMPLIANCE WITH ETHICAL STANDARDS:

Conflict of Interest: M. Kafrouni is an employee of DOSIsoft SA (Cachan, France) as a PhD student. S. Vauclin is an employee of DOSIsoft SA (Cachan, France). The other authors declare that they have no conflicts of interest.

12

Ethical approval: All procedures were performed in accordance with the ethical standards of the institutional and national research committee, and the Declaration of Helsinki.

REFERENCES

1. Cremonesi M, Chiesa C, Strigari L, et al. Radioembolization of hepatic lesions from a radiobiology and dosimetric perspective. *Front Oncol*. 2014;4:210.

2. The Package Insert for SIR-Spheres®. Accessed on https://www.sirtex.com/media/155127/pi-ec-12.pdf. Sirtex Medical Limited, New South Wales, Australia. 2017.

3. Kao YH, Tan EH, Ng CE, Goh SW. Clinical implications of the body surface area method versus partition model dosimetry for yttrium-90 radioembolization using resin microspheres: a technical review. *Ann Nucl Med*. 2011;25:455-461.

4. Lam MG, Louie JD, Abdelmaksoud MH, Fisher GA, Cho-Phan CD, Sze DY. Limitations of body surface area-based activity calculation for radioembolization of hepatic metastases in colorectal cancer. *J Vasc Interv Radiol*. 2014;25:1085-1093.

5. Smits MLJ, Elschot M, Sze DY, et al. Radioembolization dosimetry: the road ahead. *Cardiovasc Intervent Radiol*. 2015;38:261-269.

6. Traino AC, Boni G, Mariani G. Radiodosimetric estimates for radioembolic therapy of liver tumors: challenges and opportunities. *J Nucl Med*. 2012;53:509-511.

7. Kennedy A, Coldwell D, Sangro B, Wasan H, Salem R. Radioembolization for the treatment of liver tumors: general principles. *Am J Clin Oncol*. 2012;35:91–99.

8. Bolch WE, Bouchet LG, Robertson JS, et al. MIRD Pamphlet No. 17: the dosimetry of nonuniform activity distributions - radionuclide S values at the voxel level. Medical Internal Radiation Dose Committee. *J Nucl Med*. 1999;40:11S-36.

9. Forner A, Ayuso C, Varela M, et al. Evaluation of tumor response after locoregional therapies in hepatocellular carcinoma: are response evaluation criteria in solid tumors reliable? *Cancer*. 2009;115:616-623.

10. Lau WY, Kennedy AS, Kim YH, et al. Patient selection and activity planning guide for selective internal radiotherapy with yttrium-90 resin microspheres. *Int J Radiat Oncol Biol Phys*. 2012;82:401-407.

11. Keppke AL, Salem R, Reddy D, et al. Imaging of hepatocellular carcinoma after treatment with yttrium-90 microspheres. *AJR Am J Roentgenol*. 2007;188:768-775.

12. Strigari L, Sciuto R, Rea S, et al. Efficacy and toxicity related to treatment of hepatocellular carcinoma with 90Y-SIR spheres: radiobiologic considerations. *J Nucl Med*. 2010;51:1377-85.

13. Kao YH, Lichtenstein M. Origin, dosimetric effect and clinical limitations of the semi-empirical body surface area method for radioembolisation using yttrium-90 resin microspheres. *J Med Imaging Radiat Oncol*. 2016;60:382-385.

14. Grosser OS, Gerhard U, Furth C, et al. Intrahepatic activity distribution in radioembolisation with yttrium-90-labeled resin microspheres using the body surface area method-a less than perfect model. *J Vasc Interv Radiol*. 2012;26:1615-1621.

15. Samim M, van Veenendaal LM, Braat MN, et al. Recommendations for radioembolisation after liver surgery using yttrium-90 resin microspheres based on a survey of an international expert panel. In press, *Eur Radiol*. 2017.

16. Dieudonne A, Garin E, Laffont S, et al. Clinical feasibility of fast 3-dimensional dosimetry of the liver for treatment planning of hepatocellular carcinoma with 90Y-microspheres. *J Nucl Med*. 2011;52:1930-7.

17. Petitguillaume A, Bernardini M, Hadid L, de Labriolle-Vaylet C, Franck D, Desbrée A. Three-dimensional personalized Monte Carlo dosimetry in 90Y resin microspheres therapy of hepatic metastases: non tumoral liver and lungs radiation protection considerations and treatment planning optimization. *J Nucl Med*. 2014;55:405-13.

18. Kao YH, Steinberg J, Tay Y, et al. Post-radioembolization yttrium-90 PET/CT-part 2: dose-response and tumor predictive dosimetry for resin microspheres. *EJNMMI Res*. 2013;3:57.

19. Fowler KJ, Maughan NM, Laforest R, et al. PET/MRI of hepatic 90Y microsphere deposition determines individual tumor response. *Cardiovasc Intervent Radiol*. 2016;39:855-64.

20. Fox RA, Klemp PF, Egan G, Mina LL, Burton MA, Gray BN. Dose distribution following selective internal radiation therapy. *Int J Radiat Oncol Biol Phys*. 1991;21:463-7.

21. Campbell AM, Bailey IH, Burton MA. Analysis of the distribution of intra-arterial microspheres in human liver following hepatic yttrium-90 microsphere therapy. *Phys Med Biol*. 2000;45:1023-33.

22. Kennedy AS, Nutting C, Coldwell D, Gaiser J, Drachenberg C. Pathologic response and microdosimetry of (90)Y microspheres in man: review of four explanted whole livers. *Int J Radiat Oncol Biol Phys*. 2004;1:1552-630.

23. D'Arienzo M, Filippi L, Chiaramida P, et al. Absorbed dose to lesion and clinical outcome after liver radioembolization with (90)Y microspheres: a case report of PET-based dosimetry. *Ann Nucl Med*. 2013;27:676.

24. Knesaurek K, Machac J, Muzinic M, DaCosta M, Zhang Z, Heiba S. Quantitative comparison of yttrium-90 (90Y)-microspheres and technetium-99m (99mTc)-macroaggregated albumin SPECT images for planning 90Y therapy of liver cancer. *Technol Cancer Res Treat*. 2010; 9:253-61.

25. Wondergem M, Smits ML, Elschot M, et al. 99mTc macroaggregated albumin poorly predicts the intrahepatic distribution of 90Y resin microspheres in hepatic radioembolization. *J Nucl Med*. 2013;54:1294-1301.

26. Chiesa C, Mira M, Maccauro M, et al. Radioembolization of hepatocarcinoma with 90-Y glass microspheres: development of an individualized treatment planning strategy based on dosimetry and radiobiology. *Eur J Nucl Med Mol Im*. 2015;42:1718-38.
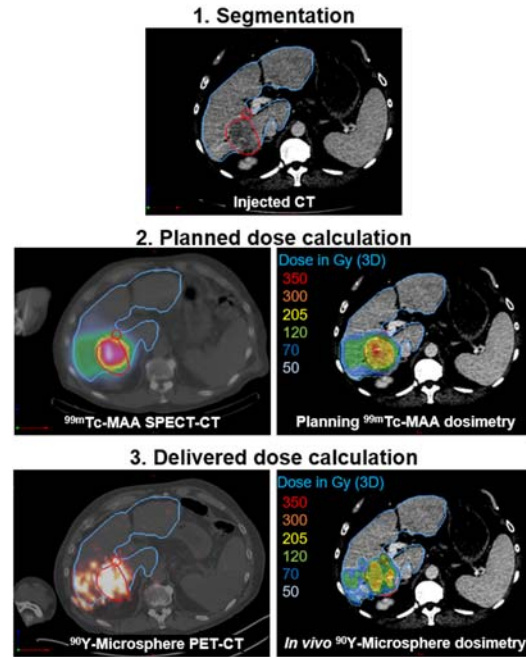
Figure 1. Process of retrospective pre and post-treatment dosimetry. Tumor and NTL are delineated in red and blue respectively.
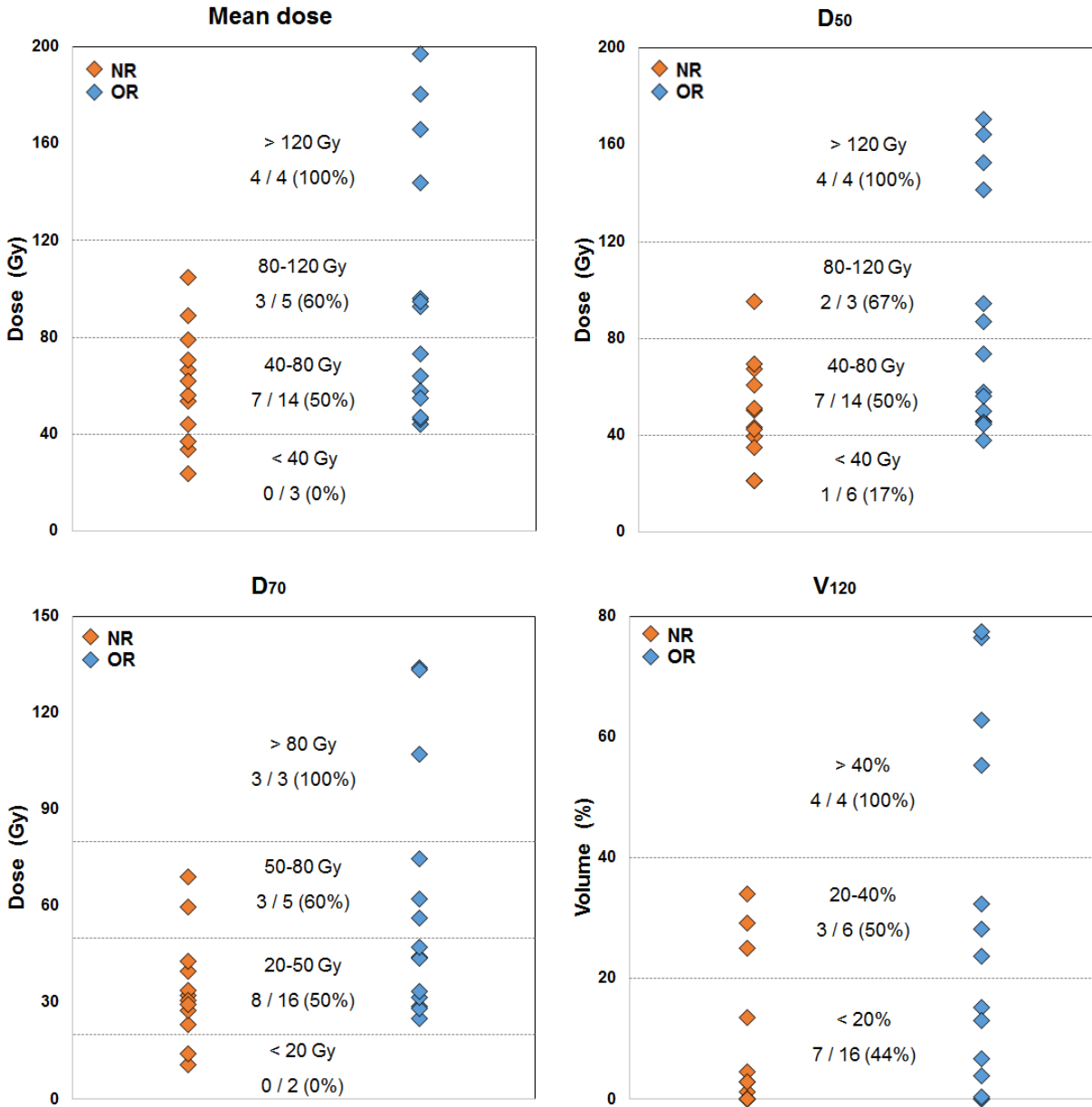
Figure 2. ^{90}Y-microsphere PET based tumor mean dose and DVH metrics in non-responding (NR, in orange) and objective response (OR, in blue) treatments. Number and percentage of responding tumors are specified for stratified ranges of dose metrics, highlighting dose-effect relationship.
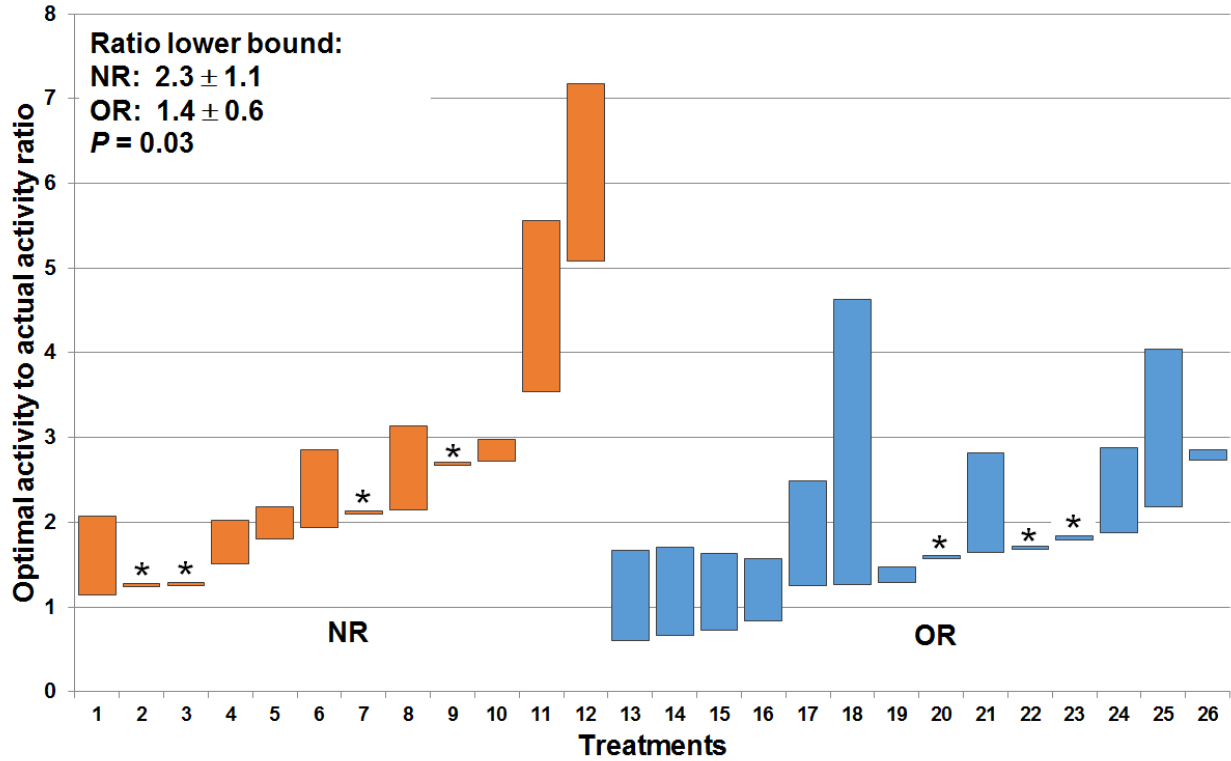
17

Figure 3. Optimal to actual (BSA-based) activity ratio for each of the 26 treatments with 6 month-EASL response evaluation. Lower bound corresponds to the 120 Gy objective to the tumor, upper bound to the 50 Gy and 30 Gy objective to NTL and lungs respectively. Treatments in which NTL and lung dose limitations would not allow to reach 120 Gy to the tumor are marked with an asterisk. OR = objective response, NR = non-responding
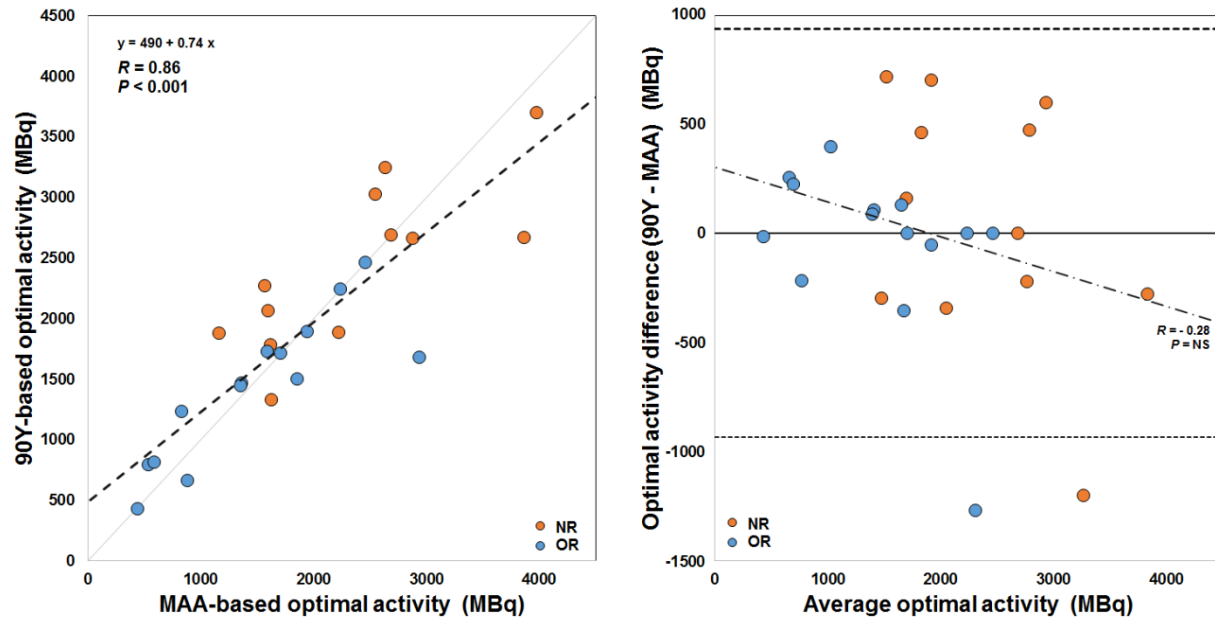
Figure 4. Comparison between the optimal activities calculated based on ^{99m}Tc-MAA and ^{90}Y-microsphere dosimetry. Left: scatter plot. The dashed line stands for the linear regression. Right: Bland-Altman diagram. The plain line indicates the mean difference and the dashed lines the 95% limits of agreement. OR = objective response in blue, NR = non-responding in orange, R: Pearson's correlation, NS = not significant.

Clinical Variable	Value
Age (years)	64 ± 11
Gender	
Male	39
Female	3
WHO performance status	
0	32
1	10
BCLC classification	
B	14
C	28
Child Classification	
A5	24
A6	12
B7	6
Prior local therapy[*]	
Yes	27
No	15
Tumor morphology	
Infiltrative	21
Nodular	21
Portal Vein Thrombosis	
Yes	21
No	21
Number of lesions (>2cm)	
1	22
>1 and <5	13
≥5	7
Tumor burden (%)	
<25	33
>25 and <50	7
>50	2

TABLE 1. Baseline Characteristics for the 42 treatments. WHO = World Health Organization. BCLC = Barcelona Clinic Liver Cancer. (*) Prior local therapies include chemoembolization, radiofrequency ablation.

	All (n=42)				OR (n=14)		NR (n=12)		
	Mean	SD	Median	Range	Mean	SD	Mean	SD	*P* (OR vs NR)
IA (GBq)	1.18	0.43	1.10	0.29-2.60	1.07	0.51	1.18	0.29	*NS*
Lung shunt (%)	6.8	4.0	5.9	1.73-18.6	6.4	4.0	6.5	3.0	*NS*
Tumor volume (cm^3)	407	462	213	8-2043	214	175	385	374	*NS*
Mean dose (Gy)									
Tumor (MAA)	77	51	52	19-212	104	58	68	41	*0.09*
Tumor (^{90}Y)	74	47	60	23-197	97	53	60	24	*0.04*
P (MAA vs ^{90}Y)	*NS*				*NS*		*NS*		
Non-tumoral liver (MAA)	16	9	17	0-38	17	7	16	9	*NS*
Non-tumoral liver (^{90}Y)	22	9	21	7-44	24	8	21	10	*NS*
P (MAA vs ^{90}Y)	*0.003*				*0.02*		*NS*		
DVH indices									
D$_{50\text{-MAA}}$ (Gy)	61	49	43	9-219	92	62	50	27	*0.04*
D$_{50\text{-90Y}}$ (Gy)	66	46	48	15-200	87	49	50	21	*0.02*
P (MAA vs ^{90}Y)	*NS*				*NS*		*NS*		
D$_{70\text{-MAA}}$ (Gy)	34	35	24	1-164	57	48	28	22	*0.06*
D$_{70\text{-90Y}}$ (Gy)	45	36	32	8-165	61	38	34	17	*0.04*
P (MAA vs ^{90}Y)	*NS*				*NS*		*NS*		
V$_{120\text{-MAA}}$ (%)	19	23	8	0-83	33	27	13	16	*0.04*
V$_{120\text{-90Y}}$ (%)	19	25	8	0-87	28	28	9	13	*0.05*
P (MAA vs ^{90}Y)	*NS*				*NS*		*NS*		

TABLE 2. Main dose metrics regarding all the evaluations included (n=42) and those for which six-month tumor response evaluation according to EASL criteria was available (n=26). OR: objective response, NR: non-responding, SD = standard deviation, IA = injected activity, NS = not significant, MAA: ^{99m}Tc-macroaggregated albumin

Retrospective voxel-based dosimetry for assessing the body surface area model ability to predict delivered dose and radioembolization outcome

Marilyne Kafrouni, Carole Allimant, Marjolaine Fourcade, Sébastien Vauclin, Julien Delicque, Alina-Diana Ilonca, Boris Guiu, Federico Manna, Nicolas Molinari, Denis Mariano-Goulart and Fayçal Ben Bouallègue

This article and updated information are available at:
http://jnm.snmjournals.org/content/early/2018/03/14/jnumed.117.202937

Information about reproducing figures, tables, or other portions of this article can be found online at:
http://jnm.snmjournals.org/site/misc/permission.xhtml

Information about subscriptions to JNM can be found at:
http://jnm.snmjournals.org/site/subscriptions/online.xhtml